Laser Diode Feedback Interferometer for Measurement of Displacements without Ambiguity

Silvano Donati, Guido Giuliani, and Sabina Merlo

Abstract— **We report what, to our knowledge, is the first example of laser feedback interferometer capable of measuring displacements of arbitrary form using a single interferometric channel. With a GaAlAs laser diode we can measure 1.2-m displacements, with interferometric resolution, simply by means of the backreflection from the surface (reflective or diffusive) under test. The operation is performed at moderate (i.e., not very weak) levels of feedback, such that a two-level hysteresis is found in the amplitude modulated signal. This is shown to allow the recovery of displacement without sign ambiguity from a single interferometric signal. Experimental results are reported, which are found to be in good agreement with the underlying theory. Performances of the developed feedback interferometer are finally presented.**

I. Introduction

When a small fraction of the power emitted from a single frequency laser is allowed to reenter the laser cavity, as in the case of a remote surface either reflective or diffusive illuminated by the laser spot, an injection modulation of the cavity field is generated, both in amplitude and frequency. The driving term of the modulation is the optical pathlength 2 ks of light to the remote target and back, where $k = 2\pi/\lambda_0$ and λ_0 is the emission wavelength of the unperturbed laser. At very weak levels of feedback the modulation indexes are in quadrature, that is cos 2 ks for the amplitude component and sin 2 ks for the frequency component. By means of these two signals it is possible to recover the displacement $\Delta s = s(t) - s_0$ from an initial position s_0 to the current position $s(t)$ without ambiguity, as in the standard double-beam laser interferometry.

Observation of amplitude modulation due to injection dates back to about 25 years ago [1], [2] when the effect was first noticed in HeNe and CO_2 lasers and then proposed as a principle for measuring remote vibrations of sub-wavelength amplitudes. The theory of injection modulation was developed shortly later by Spencer and Lamb [3] who showed that injection gives also frequency modulation and bistability.

In 1978, one of the authors [4] demonstrated the principle of injection interferometry for arbitrary displacement waveforms $s(t)$, using a dual-frequency Zeeman He-Ne laser to recover the frequency modulation component sin 2 ks by heterodyne detection with the second (fixed-frequency) mode, in addition to the amplitude component cos 2 ks available on the intensity.

Manuscript received March 25, 1993. This work was supported in part by a MURST 40% contract.

The authors are with the Dipartimento di Elettronica, Università di Pavia, via Abbiategrasso 209, I-27100 Pavia, Italy.

IEEE Log Number 9406888.

Later, even though several examples of feedback interferometry [5]–[12] applied to small vibrations detection, ranging, and velocimetry have been reported using laser diodes, the efforts of developing a true unambiguous interferometric readout of ks have been hindered by the excessive frequency linewidth of laser diodes (even in stabilized units), and by the requirement of having a second identical source (unperturbed by feedback) to be used as the local oscillator for the detection of the frequency deviation of the perturbed source.

Thus, up to now, the only available signal in an injection interferometer was the amplitude component cos 2 ks, easily picked out from the intensity, and sufficient for measuring vibrations of small ($<\lambda/4$) amplitudes. To this end, the interferometer is stabilized at the half-fringe condition through an added s', so that $s = \Delta s + s'$, $s' = \lambda/4$ and $\cos 2\ ks = \sin 2\ k\Delta s \approx 2k\Delta s$ for small Δs.

Now, an interesting question can be raised: which class of functions $s(t)$ can be reconstructed exactly (at least in principle) from a measured function $F(t) = \cos 2\ ks(t)$? Let us exclude the linearity error of the cosine function, easily corrected by post-distorsion through the arccosine function, and focus on the ambiguity which occurs when the argument of cosine reaches π or multiples of it, where one cannot tell whether the signal is increasing or decreasing. Reversing the argument, a class of signals excaping the ambiguity is clearly that of monotonic signals, for which one can get the true signal as

$$s(t) = (1/2k)[\arccos F(t) + n\pi] \tag{1.1}$$

where n is increased or decreased by one at each zero-derivative point found in $F(t)$, for positive or negative slope signals, respectively.

Developing this point further, it is straightforward to think of a scheme for circumventing the ambiguity: we add a ramp signal $r(t) = Ht$ to $s(t)$ in order to have a monotonic result $r(t) + s(t)$, and after reconstruction we will subtract $r(t)$ to get the result. In principle, this leads to the correct reconstruction of all waveforms belonging to the class of signals with slope less than H.

To avoid the practical difficulty of $r(t)$ getting too large, we can use a triangular waveform $\mathrm{tr}(t) = Ht\ (0 < t < T/2)$, $= H(T - t)\ (T/2 < t < T)$ of period T and of large amplitude, $HT/2 \gg 1/2k$. Now, (1.1) should be modified by reversing the sign of the added counting at each zero-derivative point in the alternate semiperiods (odd or even) of $\mathrm{tr}(t)$. This scheme again leads to the reconstruction of signals with slope less than H. The above scheme identifies a sort

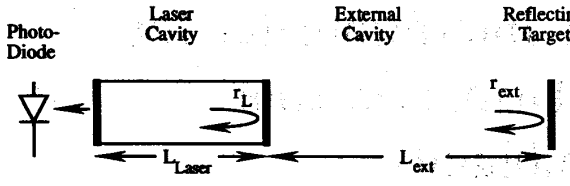

Fig. 1. Scheme of the feedback interferometer with semiconductor laser.

of dithering of the pathlength ks. Dithering can take different forms and can be implemented by mounting the laser diode on a mechanical actuator (e.g., a piezoceramic) to which the dither signal is applied or by modulating the injection current. The dither avoids ambiguity and the added signal is canceled by electronic processing of the measured signal.

However, it would be even more interesting if the laser diode itself could perform a sort of dithering. This can indeed be done in the feedback modulation regime, by moving away from the very weak level, which gives a signal approximately of the form $F = \cos 2\,\mathrm{ks}(t)$, up to the moderate level where the function F becomes more and more distorted (already noted in [13]) and similar to a sawtooth, until it exhibits fast switchings with hysteresis. These switchings occur periodically, with a period $\Delta s = \lambda_0/2$, and are upward and downward for, respectively, decreasing and increasing Δs. Therefore, it is easy to recover Δs in steps of $\lambda_0/2$ without ambiguity through an up/down counter. It is worthy to note that the transitions are independent from the signal slope, so that no constraint is imposed on the rate of rise of $s(t)$ up to the limit of the switching time.

If $D(2\,\mathrm{ks})$ is the distorted cosine function relating the optical pathlength to the measured signal amplitude F, and if we assume that the function D is bounded between -1 and $+1$ and is periodic, in particular $D(2\,\mathrm{ks}) = D(2\,\mathrm{ks} + n2\pi)$, then Eq. (1.1) modifies as follows:

$$s(t) = (1/2k)[D^{-1}(F) + n2\pi] \tag{1.2}$$

where now n is the number of counted switchings (taking the downwards as positive and the upwards as negative).

In the following, we will review the relevant injection modulation theory, find the analytical expression for D^{-1}, show the range of feedback levels which give the desired hysteresis operation, report data on the feedback modulation of our laser diode, and show the performances of the feedback interferometer for displacement measurements both on reflective (mirror and corner-cube) and diffusive targets.

II. Theory of Operation of Diode Laser Feedback Interferometer

We represent the feedback interferometer with a semiconductor laser as in Fig. 1. Radiation emitted by the laser propagates freely in the external cavity up to the remote reflecting (and movable) target, which injects a fraction of the output power back into the laser cavity. The photodiode at the rear mirror monitors the output power by means of the photogenerated current $I = \sigma P$, σ being the photodiode spectral responsivity. Modulation of the laser electric field $E_0(t)$ is induced by the variations of the external cavity length. The dynamics of the system is described by the well-known equations derived by Lang and Kobayashi [14]:

$$\frac{d}{dt}E_0(t) = \frac{1}{2}[G_N(N(t) - N_0) - 1/\tau_P]E_0(t) + \frac{\kappa}{\tau_L}E_0(t-\tau) \times \cos[\omega_0\tau + \phi(t) - \phi(t-\tau)] \tag{2.1}$$

$$\frac{d}{dt}\phi(t) = \frac{1}{2}\alpha G_N[N(t) - N_T] - \frac{\kappa}{\tau_L}\frac{E_0(t-\tau)}{E_0(t)}\sin[\omega_0\tau + \phi(t) - \phi(t-\tau)] \tag{2.2}$$

$$\frac{d}{dt}N(t) = R_P - \frac{N(t)}{\tau_S} - G_N[N(t) - N_0]E_0^2(t) \tag{2.3}$$

where we have neglected contributions coming from nonlinear gain suppression, spontaneous emission, and multiple reflections, and where we have used the following standard symbolism:

- $E(t)$ laser electric field, expressed as $E(t) = E_0(t) \times \exp[j(\omega_0 t + \phi(t))]$ with $E_0(t)$ normalized so that $E_0^2(t)$ is the photon density in the laser cavity;
- ω_0 angular frequency of the unperturbed laser;
- G_N modal gain coefficient (typical value $G_N = 8 \cdot 10^{-13}\ \mathrm{m^3 s^{-1}}$);
- $N(t)$ average carrier (electron-hole pairs) density in the active layer;
- N_0 carrier density at transparency (typical value $N_0 = 1.4 \cdot 10^{24}\ \mathrm{m^{-3}}$);
- N_T carrier density at threshold for the unperturbed laser (typical value $N_T = 2.3 \cdot 10^{24}\ \mathrm{m^{-3}}$);
- τ_P photon lifetime (typical value $\tau_P = 1.6$ ps) and $1/\tau_P = G_N(N_T - N_0)$;
- τ_L diode cavity round trip time (for our laser $\tau_L = 8.3$ ps since the mode spacing is 120.41 GHz);
- τ external cavity round trip time;
- τ_S carrier lifetime (typical value $\tau_S = 2$ ns);
- R_P electric pumping term, which is given by $R_P = J\eta/ed$, with J injected current density, η conversion efficiency, e electron charge, d active layer thickness;
- α linewidth enhancement factor defined as $\alpha = (\partial\chi_R/\partial N)/(\partial\chi_I/\partial N)$ with $\chi = \chi_R - i\chi_I$ complex susceptibility (α is usually between 3 and 7: we assume $\alpha = 6$ [15]);
- κ feedback parameter which is given, for a Fabry-Perot laser, by $\kappa = \varepsilon\kappa_{ext}$ where $k_{ext} = (1 - r_L^2)r_{ext}/r_L$ with r_L laser-facet field-reflectivity ($r_L \approx 0.56$), r_{ext} external mirror reflectivity, and ε is the coupling efficiency which takes into account the mode mismatch and the finite coherence length (typical values $\varepsilon = 0.1 \div 0.6$).

We now find the analytical expression which relates the laser output power (proportional to $E_0(t)^2$) in presence of feedback to the external cavity round trip phase $\omega_0\tau = 2$ ks.

Stationary solutions of (2.1)–(2.3) are found by taking $E_0(t) = E_F$ = constant, $N(t) = N_F$ = constant. Moreover, since the instantaneous optical frequency is given by $\omega(t) = \omega_0 + [d\phi(t)/dt]$, the contribution $d\phi(t)/dt$ represents

a frequency deviation and we can thus take $\phi(t) = (\omega_F - \omega_0)t$, where $\omega_F = \omega_F(\tau)$ is the angular frequency of the laser with external feedback [15]. By substituting into (2.1) we obtain

$$N_F = N_T - \frac{2\kappa}{G_N \tau_L} \cos \omega_F \tau \tag{2.4}$$

which shows that in presence of feedback there is also a modulation of the carrier density.

By substitution of (2.4) into (2.2), we obtain the following relationship

$$\omega_0 = \omega_F + \frac{\kappa}{\tau_L}(\alpha \cos \omega_F \tau + \sin \omega_F \tau) \tag{2.5}$$

which corresponds to the well known round trip phase change condition $\Delta\phi = 0$ [15]. For weak to moderate feedback, the allowed oscillation frequencies ω_F are solutions of the (2.5) and correspond to the external cavity modes. By introducing the feedback parameter C [15], [16]

$$C = \frac{\kappa \tau \sqrt{1+\alpha^2}}{\tau_L}. \tag{2.6}$$

Equation (2.5) can be rewritten as follows

$$\omega_0 \tau = \omega_F \tau + \frac{C}{\sqrt{1+\alpha^2}}(\alpha \cos \omega_F \tau + \sin \omega_F \tau) \tag{2.7}$$

or

$$\omega_0 \tau = \omega_F \tau + C \sin(\omega_F \tau + \arctan \alpha) \tag{2.8}$$

As already reported by other authors [15], [16], (2.8) has just one solution for ω_F when $C < 1$ and multiple solutions when $C > 1$; thus we can take the condition $C = 1$ as the boundary between the weak and the moderate feedback regime.

We now obtain the expression for the electric field E_F^2 from (2.3) using (2.4)

$$E_F^2 = \frac{R_P - (N_F/\tau_S)}{G_N(N_F - N_0)} = \frac{R_P \tau_S - N_T + \frac{2\kappa}{G_N \tau_L} \cos \omega_F \tau}{1 - \frac{2\kappa \tau_P}{\tau_L} \cos \omega_F \tau} \left(\frac{\tau_P}{\tau_S}\right). \tag{2.9}$$

Limiting our treatment to the practical case $\kappa < 0.01$, (2.9) can be approximated as follows

$$E_F^2 = \frac{\tau_P}{\tau_S}\left(R_P \tau_S - N_T + \frac{2\kappa}{G_N \tau_L} \cos \omega_F \tau\right) \times \left(1 + \frac{2\kappa \tau_P}{\tau_L} \cos \omega_F \tau\right). \tag{2.10}$$

Indicating with E_{NF} the stationary electric field in case of no feedback, which is given by

$$E_{NF}^2 = \tau_P[R_P - (N_T/\tau_S)] \tag{2.11}$$

and neglecting second-order contributions, we obtain from (2.10) the output power variation ΔP due to feedback with respect to the unperturbed laser

$$\Delta P \propto E_F^2 - E_{NF}^2 = \tau_P(R_P - N_0/\tau_S)\frac{2\kappa \tau_P}{\tau_L} \cos \omega_F \tau, \tag{2.12}$$

which can be better written, assuming that κ does not depend on the external cavity length, as

$$\Delta P = \Delta P_{\max} \cos \omega_F \tau \tag{2.13}$$

(In practice, a weak dependence of κ from τ does exist through the coupling efficiency ε).

The analytical expression for the laser output power variations in presence of feedback, as a function of the external cavity round-trip phase $\omega_0 \tau$, can then be obtained by combination of (2.7) and (2.13):

$$\omega_0 \tau = \arccos\left(\frac{\Delta P}{\Delta P_{\max}}\right) + \frac{C}{\sqrt{1+\alpha^2}} \times \left[\alpha\left(\frac{\Delta P}{\Delta P_{\max}}\right) + \sqrt{1 - \left(\frac{\Delta P}{\Delta P_{\max}}\right)^2}\right] + m2\pi \quad 0 < \omega_F \tau < \pi \tag{2.14a}$$

$$\omega_0 \tau = -\arccos\left(\frac{\Delta P}{\Delta P_{\max}}\right) + \frac{C}{\sqrt{1+\alpha^2}} \times \left[\alpha\left(\frac{\Delta P}{\Delta P_{\max}}\right) - \sqrt{1 - \left(\frac{\Delta P}{\Delta P_{\max}}\right)^2}\right] + (m+1)2\pi \quad -\pi < \omega_F \tau < 0 \quad m = 0, 1, 2, \cdots. \tag{2.14b}$$

Equations (2.14) have been found as stationary solutions and give the output power for different values of the external cavity length. We suppose now to change the cavity length in a quasi-stationary way, by imposing to the external reflector a slowly varying displacement waveform $s(t)$. From the variation $\Delta P(t)$ in the output power we determine the function $F(t) = \Delta P(t)/\Delta P_{\max}$ and use (2.14) to reconstruct $s(t)$ as follows:

$$s(t) = \left(\frac{1}{2k}\right)\left\{\arccos(F(t)) + \frac{C}{\sqrt{1+\alpha^2}} \times [\alpha F(t) + \sqrt{1 - F^2(t)}] + m2\pi\right\} \left(\frac{dF}{dt}\right) \cdot \left(\frac{ds}{dt}\right) < 0 \tag{2.15a}$$

$$s(t) = \left(\frac{1}{2k}\right)\left\{-\arccos(F(t)) + \frac{C}{\sqrt{1+\alpha^2}} \times [\alpha F(t) - \sqrt{1 - F^2(t)}] + (m+1)2\pi\right\} \left(\frac{dF}{dt}\right) \cdot \left(\frac{ds}{dt}\right) > 0 \quad m = 0, 1, 2, \cdots. \tag{2.15b}$$

In (2.15), m is increased or decreased by 1 if $ds/dt > 0$ or $ds/dt < 0$, respectively, and m is updated every two zero crossings of $F(t)$. The information about the sign of ds/dt is also contained in $F(t)$.

III. Experimental Results

Experimental results were obtained with a Mitsubishi ML2701 AlGaAs Fabry–Perot (single longitudinal mode) laser, with threshold current of 18 mA, emission wavelength 854 nm at a biasing current of 43 mA yielding up to 8 mW output power. The laser was usually operated at $I_{Bias} = 40$ mA (output power 6.7 mW) since at that current no mode hopping between longitudinal modes was observed in the working range of feedback levels.

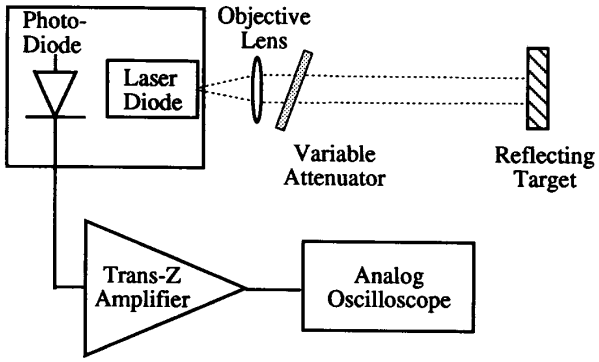

Fig. 2. Schematic diagram of the experimental optical set-up.

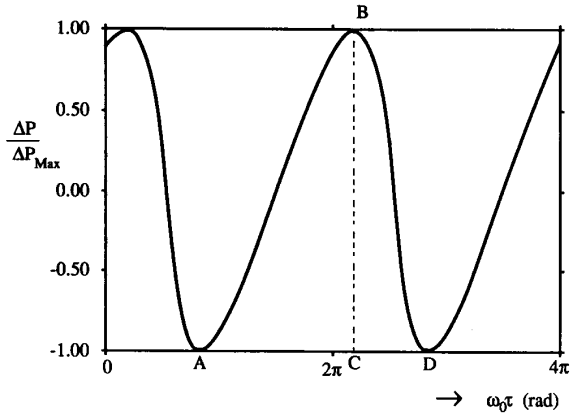

Fig. 3. The theoretical function $\Delta P/\Delta P_{\max}$ versus $\omega_0\tau$ is plotted for $C = 0.6$.

The optical set-up presented in Fig. 2 was used. Light emitted from the laser was collimated on the reflecting target (which for this set of measurements was either a mirror or a corner-cube) by means of a high numerical aperture (N.A. = 0.45) objective lens with antireflection coating at 850 nm. An attenuator with variable transmittance from 0.01 to 0.8 was inserted in the optical path so that various feedback levels could be obtained. Therefore, for this set-up κ_{ext} includes attenuator trasmissivity as well as target reflectivity. Backreflections from the attenuator were never coupled back into the laser cavity since the attenuator was slightly tilted. For the photodetection we used the photodiode incorporated into the laser package.

The comparison between the experimental and the theoretical results is now reported for weak ($C \leq 1$) and moderate ($C > 1$) feedback.

Weak feedback level: For $C \leq 1$, (2.8) yields a single-valued function $\omega_F\tau$ versus $\omega_0\tau$ with period 2π. As a consequence, also $\Delta P/\Delta P_{\max}$ as a function of $\omega_0\tau$, defined by (2.14), is single-valued, has a 2π periodicity, and assumes all the values between -1 and 1. As an example, in Fig. 3 the ratio $\Delta P/\Delta P_{\max}$ versus $\omega_0\tau$ is plotted for $C = 0.6$.

Experimentally, when a displacement $s(t)$ is applied to the reflecting target, the photodetected current $I(t)$ has the same waveform as the theoretical function $F(t)$ given by (2.15)

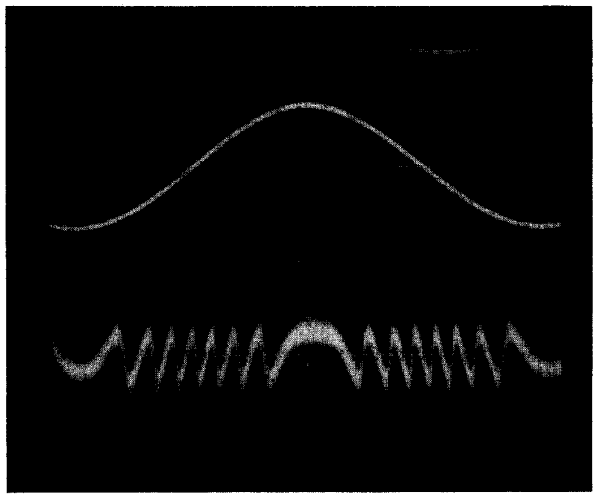

Fig. 4. Experimental results for weak injection ($C < 1$). Upper trace: drive signal $s(t)$, 20 mV/div corresponding to 1.25 μm/div; lower trace: photodetected signal of the distorted cosine without switchings, 5 mV/div. Time base: 2 ms/div.

with a peak-to-peak amplitude $\Delta I_{\text{PP}} = 2\sigma\Delta P_{\max}$. Since $I(t)$ is not symmetric, we can distinguish between $ds(t)/dt > 0$ and $ds(t)/dt < 0$. For a ramp-like displacement, $s(t) = h\ t$, $F(t)$ is proportional to $(\Delta P/\Delta P_{\max})$ $(\omega_0\tau)$ and is periodic in time with period $T = \pi/kh$.

In Fig. 4, a picture taken from the oscilloscope is presented, which shows $I(t)$ when $s(t)$ is a sinusoidal waveform. These data were collected by attaching a small mirror onto a loudspeaker, driven by a generator at $f = 50$ Hz.

By comparing experimental waveforms of the photodetected current for different attenuation levels with the theoretical behaviour at different values of C, we found that the condition $C \approx 1$ corresponds to $\kappa_{\text{ext}} \approx 1 \cdot 10^{-3}$ and $L_{\text{ext}} = 0.6$ m, which yield $\varepsilon \approx 0.34$ and $\kappa \approx 3.4 \cdot 10^{-4}$. Measurements of κ_{ext} under various coupling conditions were carried out by means of an optical power meter placed alternatively at both sides of a beamsplitter inserted between the lens and the attenuator. In this weak feedback regime, the value of C was evaluated from the shape factor $F = \text{AC/AD}$ of the function $\Delta P/\Delta P_{\max}$ shown in Fig. 3.

We also verified that ΔI_{PP} increased when κ was increased, as predicted by (2.12). This observation was done by reducing the attenuation, without leaving the weak feedback regime. Moreover, the peak-to-peak current followed small variations of injection current around the biasing condition.

Moderate feedback level: For $C > 1$, the function $\omega_F\tau$ versus $\omega_0\tau$, exhibits bistability (and for $C > 4.6$ multistability). For $1 < C < 4.6$, there is an interval of $\omega_0\tau$ in which the ratio $\Delta P/\Delta P_{\max}$ may assume three different values: two of them are stable points for the system and one is unstable. As an example, in Fig. 5(a) the theoretical function $\Delta P/\Delta P_{\max}$ versus $\omega_0\tau$ is plotted for $C = 3$.

Actually, the waveform of the photodetected current follows the evolution depicted in Fig. 5(b). Starting from point A, as $\omega_0\tau$ increases, the signal increases along the theoretical solution until it reaches point B, where it switches downward

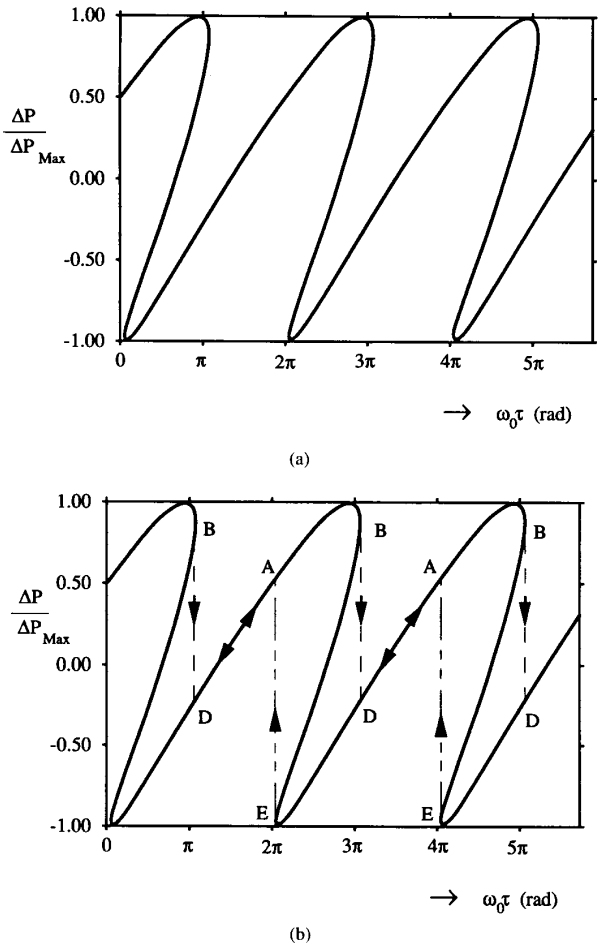

Fig. 5. (a) The theoretical function $\Delta P/\Delta P_{\max}$ versus $\omega_0 \tau$ is plotted for $C = 3$. (b) Signal path with hysteresis.

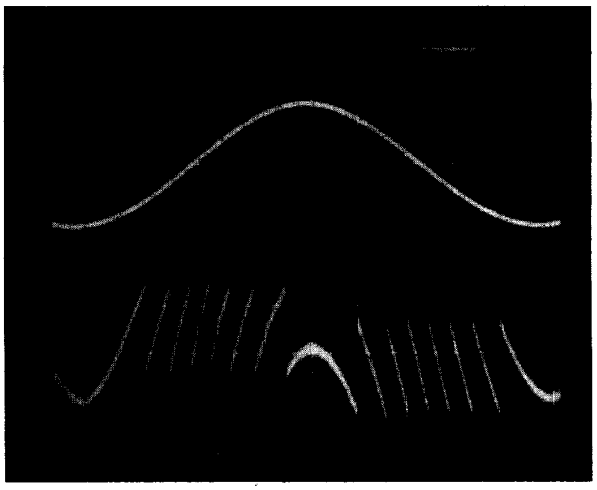

Fig. 6. Experimental results for moderate feedback. Upper trace: drive signal $s(t)$, 20 mV/div corresponding to 1.25 μm/div; lower trace: photodetected signal of the distorted cosine with switchings and hysteresis, 10 mV/div. Time base: 2 ms/div.

to D and starts to increase again until the next B point (after 2π). On the other hand, as $\omega_0\tau$ decreases, the signal exhibits upward switchings from E to A. Such a hysteresis means that the photodetected signal will be different for increasing or decreasing $s(t)$. We have investigated these characteristics for different feedback levels and various displacement waveforms $s(t)$. The ac-coupled photodetected current exhibits, with periodicity $2k\Delta s = 2\pi$, zero crossings with a very steep slope, negative if $s(t)$ is increasing and positive if $s(t)$ is decreasing. Since this switching occurs every time the external cavity length is changed by $\lambda_0/2$, by differentiating the photogenerated signal, we can obtain a positive pulse if the external cavity length is decreased by $\lambda_0/2$ and a negative pulse if it is increased by $\lambda_0/2$.

In Fig. 6, we present a picture from the oscilloscope which clearly shows the sawtooth-like behaviour of the photogenerated current and the strong hysteresis when $s(t)$ is a sinusoid. Because of the hysteresis, when the displacement is oscillating around a fixed position, it is possible to identify in the photodetected current an upper signal level (corresponding to the path DB in Fig. 5(b)) which is the stable solution for increasing cavity length and a lower signal corresponding to the path AE which is the stable solution for decreasing cavity length. If we now take ΔI_{PP} as the difference between the highest peak of the upper level and the lowest peak of the lower level, we easily verify again that ΔI_{PP} increases when κ is increased. By comparing experimental waveforms of the photodetected current with the theoretical behaviour at different values of C, we have found that the condition $C \approx 4.6$ is obtained for $\kappa_{\mathrm{ext}} \approx 4.7 \cdot 10^{-3}$ and $L_{\mathrm{ext}} = 0.6$ m, that is $\kappa \approx 1.7 \cdot 10^{-3}$. (The value of the C parameter was obtained by taking into account the relative amplitudes of upper and lower signal level, and the hysteresis width.)

Therefore, if $C > 1$ the photodetected current, normalized to the peak-to-peak value, might be used to reconstruct $s(t)$ through (2.15), increasing m for every negative pulse and decreasing it for positive pulses.

More interesting for practical applications, when $C > 1$ the value of a displacement $\Delta s(t)$ with sign can be easily estimated with a resolution of $\lambda_0/2$ by counting the pulses, that are generated when the photodetected signal is differentiated, with an up-down counter according to the polarity of the pulses. This system will be described in detail in Section IV.

We now wonder which is the highest value of C that will assure the presence of a pulse for every $\lambda_0/2$ change in external cavity length. When $C > 4.6$, multistability is predicted by the theory and the function $\Delta P/\Delta P_{\max}$ as given by (2.14) assumes five different values. This situation is depicted in Fig. 7, where in addition to transitions BD and EA, also the transitions BD′ and EA′ are possible. However, we observed experimentally that such transitions did not occur if κ was smaller than a critical value κ^*, even though $C > 4.6$. Our results are in agreement with the observation [15] that for $\kappa < \kappa^*$ only the external cavity mode with the lowest spectral linewidth can oscillate. A further increase in feedback brings the laser in the regime where multistability does occur.

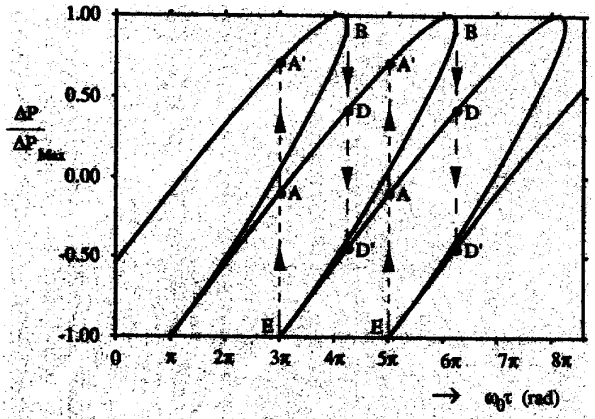

Fig. 7. Theoretical function $\Delta P/\Delta P_{max}$ versus $\omega_0\tau$ for $C = 6$ with the path related to multistability.

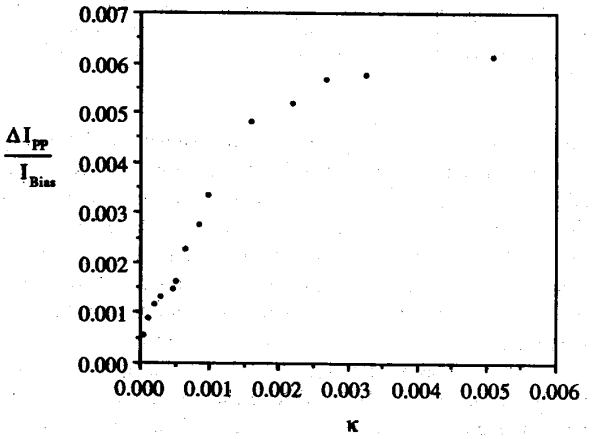

Fig. 8. Experimental results for $\Delta I_{PP}/I_{Bias}$ versus feedback parameter κ, showing the saturation for high κ.

We found that for $\kappa > \kappa^* \approx 3 \cdot 10^{-3}$, zero crossings with a very steep slope do not occur every time the external cavity length is changed by $\lambda_0/2$, but randomly some switchings are lost. We also observed that as soon as multistability shows up, the peak-to-peak current saturates, as shown in Fig. 8. Therefore, the saturation is reported at the highest feedback level that can be tolerated in the interferometer in order to have a number of switchings which actually corresponds to the overall displacement.

IV. Single-Channel Displacement Measurements

Using the diode laser feedback interferometer working in the bistable regime with hysteresis, we have implemented a compact instrument that is able to measure the value of a displacement $\Delta s(t)$ with sign in steps of $\lambda_0/2$. The interferometer sets no constraints on the waveform of displacement (that can be also nonmonotonic) and supplies the sign of it.

The optical set-up used for displacement measurements is simply made by the laser, a collimating optics, and a variable attenuator (Fig. 9). The electronic circuit for signal processing includes a differentiator (high-pass filter), which

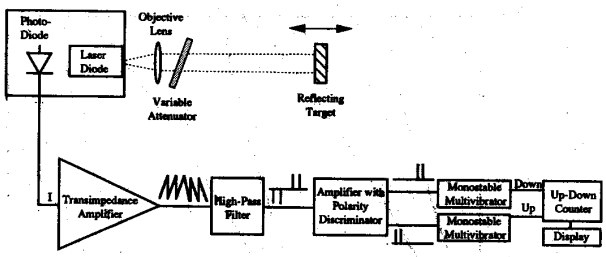

Fig. 9. Block diagram of the feedback interferometer with semiconductor laser for displacement measurements.

provides positive and negative pulses at the fast transitions of the photodetected signal, and an amplifier capable of discriminating the pulse polarity. An up-down counter with a 5-digit display accumulates the countings which give the displacement in $\lambda_0/2$ units. With this experimental configuration, we investigated the range of operation in terms of working distance and required attenuation, as well as the accuracy.

First, we tested the interferometer onto a small mirror mounted on a loudspeaker, driven by a generator. The variable attenuator was adjusted in order to obtain a photodetected signal in the typical range $C = 1 \div 4.6$ so that the hysteresis error in displacement is less than $\lambda_0/2$. Correct operation of the interferometer was verified by checking that the average value on the display remained constant while the optical pathlength was modulated by means of the loudspeaker.

Then, we mounted the reflecting target, either a small mirror or a corner-cube, on a movable holder, actuated by a high-precision micrometer with 1-μm resolution and 11-mm dynamic range with side stops. A 10-mm displacement, aligned parallel to the direction of propagation of the laser beam, was performed several times forward and backward at different distances, and the number of countings was recorded. The total number of countings resulted ± 23420, thus yielding an experimental resolution of $\lambda_0/2 \approx 427$ nm. The interferometer worked properly for target distances up to 2.5 m.

Since the rate of switchings to be counted is proportional to the derivative of $s(t)$, the maximum working frequency f_{max} of the electronics determines an upper limit to the target velocity, as $v_{max} = f_{max}\lambda_0/2$ (in our case $f_{max} = 50$ kHz so that $v_{max} = 21.35$ mm/s).

An important feature of the interferometer is the dynamic range, that is the maximum displacement of the target that allows proper operation without changing the attenuation or the focusing distance. With the reflecting target, we have obtained a maximum dynamic range of about 1.2 m.

We tested the instrument also on a diffusive target for which the backreflected field is in the speckle-pattern regime. Since speckle dimensions, longitudinal and trasversal, have respectively a dependance D^{-2} and D^{-1}, where D is the spot diameter on the diffusive surface, the best coupling is obtained when the laser beam is focused on the target. This condition corresponds also to minimizing the speckle-induced random error on ks [17]. In this case, we obtained suitable feedback levels in absence of the attenuator. Experimental working distances were in the range $0.1 \div 1$ m with a dynamic range of about 20 cm.

The accuracy of the laser diode interferometer is limited by the dependence of the emission wavelength on drive current and temperature. From the supplier specifications, our laser exhibits a $d\lambda/dI = 0.014$ nm/mA and a $d\lambda/dT = 0.05$ nm/°C. For a distance $L = 50$ cm, when current is stabilized within ± 10 μA and temperature within ± 0.01°C, the combined effect is a total error of ± 1 counting (≈ 0.4 μm). Although a much better result can be obtained by He-Ne based interferometer, the achieved level of accuracy (10^{-6}) is suitable for most industrial applications. A possible improvement may consist in using a DFB laser for which a long-term stability of 10^{-7} has been proved [18].

V. Conclusion

We have demonstrated a new approach to laser diode feedback interferometry. Displacement measurements without sign ambiguity are performed by counting the fast switchings in the photodetected current when the laser is operated in the moderate feedback regime. Our instrument is based on a very simple optical set-up and straightforward electronic signal processing. This compact system has a sufficiently wide range of operation to ensure measurements of 1.2-m displacements on distances up to 2.5 m. We foresee interesting applications of this instrument in industrial environment for accurate control of machinery movements.

Acknowledgment

S. Merlo and G. Giuliani wish to thank Prof. V. Annovazzi Lodi for helpful discussions and suggestions.

References

[1] M. J. Rudd, "A laser doppler velocimeter employing the laser as a mixer-oscillator," *J. Scientif. Instrum.*, vol. 1, pp. 723–726, 1968.
[2] T. E. Honeycutt and W. F. Otto, "A CO_2 Interferometer by reflected waves," *IEEE J. Quantum Electron.*, vol. QE-8, pp. 91–93, 1972.
[3] M. B. Spencer and W. E. Lamb, Jr., "Laser with a transmitting window," *Phys. Rev. A*, vol. 5, pp. 884–892, 1972.
[4] S. Donati, "Laser interferometry by induced modulation of cavity field," *J. Appl. Phys.*, vol. 49, no. 2, pp. 495–497, Feb. 1978.
[5] P. J. de Groot, G. M. Gallatin, and S. H. Macomber, "Ranging and velocimetry signal generation in a backscatter-modulated laser diode," *Appl. Opt.*, vol. 27, No. 21, pp. 4475–4480, Nov 1 1988.
[6] P. J. de Groot and G. M. Gallatin, "Backscatter-modulation velocimetry with an external-cavity laser diode," *Opt. Lett.*, vol. 14, no. 3, pp. 165–167, Feb. 1, 1989.
[7] S. Shinoara, H. Naito, H. Yoshida, H. Ikeda, and M. Sumi, "Compact and versatile self-mixing type semiconductor laser doppler velocimeters with direction discrimination circuit," *IEEE Trans. Instrum. Meas.*, vol. 38, no. 2, pp. 574–577, Apr. 1989.
[8] M. H. Koelink, M. Slot, F. F. M. de Mul, J. Greve, R. Graaff, A. C. M. Dassel, and J. G. Aarnoudse, "Laser-doppler velocimeter based on the self-mixing effect in a fiber-coupled semiconductor laser: Theory," *Appl. Opt.*, vol. 31, no. 18, pp. 3401–3408, June 20, 1992.
[9] F. F. M. de Mul, M. H. Koelink, A. L. Weijers, J. Greve, J. G. Aarnoudse, R. Graaff, and A. C. M. Dassel, "Self-mixing laser-doppler velocimetry of liquid flow and of blood perfusion in tissue," *Appl. Opt.*, vol. 31, no. 27, pp. 5844–5851, Sept. 20, 1992.
[10] K. Mito, H. Ikeda, M. Sumi and S. Shinoara, "Self-mixing effect of the semiconductor laser doppler method for blood flow measurement," *Med. & Biol. Eng. Comput.*, vol. 31, pp. 308–310, May 1993.
[11] S. Shinoara, H. Yoshida, H. Ikeda, K.-I. Nishide and M. Sumi, "Compact and high-precision range finder with wide dynamic range and its application," *IEEE Trans. Instrum. Meas.*, vol. 41, no. 1, pp. 40–44, Feb. 1992.
[12] T. Yoshino, M. Nara, S. Mnatzakanian, B. S. Lee, and T. C. Strand, "Laser diode feedback interferometer for stabilization and displacement measurements," *Appl. Opt.*, vol. 26, no. 5, pp. 892–897, March 1, 1987.
[13] V. Annovazzi Lodi and S. Donati, "Injection modulation in coupled laser oscillators," *IEEE J. Quantum Electron.*, vol. QE-16, pp. 859–865, 1980.
[14] R. Lang and K. Kobayashi, "External optical feedback effects on semiconductor injection laser properties," *IEEE J. Quantum Electron.*, vol. QE-16, no. 3, pp. 347–355, Mar. 1980.
[15] K. Petermann, *Laser Diode Modulation and Noise*. Dordrecht, The Netherlands: Kluwer Academic, 1988.
[16] G. A. Acket, D. Lenstra, A. J. Den Boef, and B. H. Verbeek, "The influence of feedback intensity on longitudinal mode properties and optical noise in index-guided semiconductor lasers," *IEEE J. Quantum Electron.*, vol. QE-20, pp. 1163–1169, Oct. 1984.
[17] S. Donati and G. Martini, "Speckle pattern intensity and phase: Second order conditional statistics," *J. Opt. Soc. Amer.*, vol. 69, pp. 1690–94, 1979.
[18] R. S. Vodhanel, M. Krain, and R. E. Wagner, "Long-term wavelength drift of 0.01 nm/yr for 15 free-running DFB laser," in *OFC-94 Tech. Dig.*, San Jose, CA, Feb. 20–25, 1994, Paper WG5, pp. 103–104.

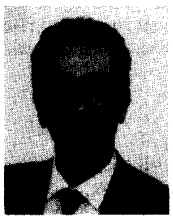

S. Donati (M'75) graduated in Physics at the University of Milano in 1966.

For nine years he was with CISE (Milano), working on noise in photomultipliers and avalanche photodiodes, nuclear electronics and electrooptic instrumentation (laser telemetry, speckle pattern interferometry, gated vision in scattering media). In 1975, he joined the Department of Electronics, University of Pavia, as internal lecturer and worked on feedback interferometers, fiber gyroscope, and noise in CCDs. In 1980, he became full Professor of Optoelectronics, and since then his main research interests have been optical fiber sensors, passive fiber components for telecommunications, free-space and guided optical interconnections, locking and chaos in lasers.

Dr. Donati has authored or coauthored about hundred papers and holds four patents. He is a member of AEI, APS, OSA, and ISHM, and has actively served to organize several national and international meetings and schools in the steering and programme committees or as a chairman. He also worked in the standardisation activity of CEI/IEC (CT-76 laser safety and CT-86 optical fibers).

G. Giuliani was born in Milano, Italy, in 1969. He graduated in Electronic Engineering from the University of Pavia, Pavia, Italy in 1993. Since November 1993, he is pursuing the Ph.D. degree in electronic engineering and computer science at the University of Pavia.

His main research interests are diode laser interferometry and optical amplifiers.

S. Merlo was born in Pavia, Italy in 1962. She graduated in Electronic Engineering from the University of Pavia, Pavia, Italy in 1987, received the M.S.E. degree in bioengineering from the University of Washington, Seattle, WA in 1989 and Ph.D. degree in electronic engineering and computer science from the University of Pavia in 1992.

Since 1993, she has been a Faculty member of the Department of Electronics at the University of Pavia. Her research work includes fiberoptic sensors for biochemical and electrical applications; advanced photodetection techniques and all-fiber passive components for telecommunications and sensors; laser interferometry.